Fundamentals of the adhesion of physical vapor deposited ZnMg-Zn bilayer coatings to steel substrates

Sabooni, Soheil; Ahmadi, Masoud; Galinmoghaddam, Emad; Westerwaal, R. J.; Boelsma, C; Zoestbergen, Edzo; Song, G.M; Pei, Yutao T.

Published in:
Materials & design

DOI:
10.1016/j.matdes.2020.108560

Publication date:
2020

Materials and Design 190 (2020) 108560

Contents lists available at ScienceDirect

Materials and Design

journal homepage: www.elsevier.com/locate/matdes

Fundamentals of the adhesion of physical vapor deposited ZnMg-Zn bilayer coatings to steel substrates

S. Sabooni [a], M. Ahmadi [a], E. Galinmoghaddam [a], R.J. Westerwaal [b], C. Boelsma [b], E. Zoestbergen [b], G.M. Song [c], Y.T. Pei [a,*]

[a] Department of Advanced Production Engineering, Engineering and Technology Institute Groningen, University of Groningen, Nijenborgh 4, 9747 AG Groningen, the Netherlands
[b] Tata Steel Nederland Technology B.V., P.O. Box 1000, 1970 CA IJmuiden, the Netherlands
[c] Schunk Xycarb Technology, Zuiddijk 23, 5705 CS Helmond, the Netherlands

HIGHLIGHTS

- The fundamentals of adhesion of ZnMg-Zn coated steels are investigated.
- The work of adhesion at the ZnMg/Zn interface is lower than that of Zn/steel interface.
- Interfacial adhesion strength depends mostly on Mg concentration and the density of interfacial defects.
- Adhesion performance of ZnMg-Zn coatings depends on both the interfacial adhesion strength and the thickness of bi-layers.
- There are threshold values for the thickness of Zn and ZnMg layers for optimum performance.

GRAPHICAL ABSTRACT

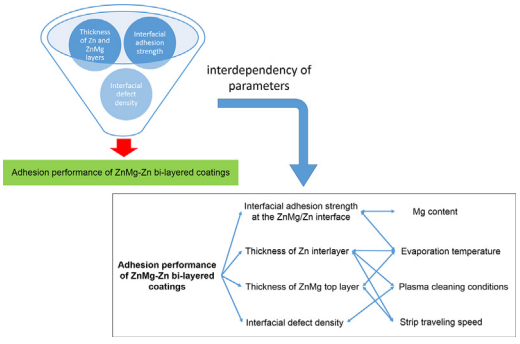

ARTICLE INFO

Article history:
Received 29 October 2019
Received in revised form 14 January 2020
Accepted 7 February 2020
Available online 8 February 2020

Keywords:
ZnMg coatings
Physical vapor deposition
Adhesion performance
Interfacial adhesion strength
Scratch test

ABSTRACT

In the present study, ZnMg-Zn bilayer coatings with different Mg concentrations and layer thicknesses are deposited on steel substrates by a thermal evaporation process. Thermodynamic calculations reveal that the work of adhesion at the ZnMg/Zn interface (~1.6 J/m^2) is lower than that at the Zn/Steel interface (~3 J/m^2). This indicates that the ZnMg/Zn interface is inherently weaker than the interface between Zn and steel substrate. The interfacial adhesion strength quantified by the scratch test shows that the adhesion strength at the ZnMg/Zn interface decreases with increasing the Mg content and reaches 66 MPa at 16.5 wt% Mg. It is found that the presence of interfacial defects largely decreases the adhesion strength compared to a defect-free coating. Meanwhile, it is also concluded that the interfacial adhesion strength at the ZnMg/Zn interface does not depend on the thickness of Zn interlayer. The results of the present investigation show that the interfacial adhesion strength is not the only governing parameter for the adhesion performance of the ZnMg-Zn bilayer coatings in forming process, but the thickness of the layers as well as interfacial defect density also play important roles in the adhesion performance.

* Corresponding author.
E-mail address: Y.Pei@rug.nl (Y.T. Pei).

https://doi.org/10.1016/j.matdes.2020.108560

1. Introduction

In the automotive industry, the protection of the vehicle body from atmospheric corrosion is generally obtained by zinc coatings [1]. Recently, it has been observed that the addition of alloying elements such as Ni, Mn, Al and Mg to the pure zinc increases its corrosion performance to a great extent [2–5]. The higher corrosion resistance of ZnMg coatings is related to the formation of a dense corrosion product called "simonkolleite" in the presence of Mg rather than ZnO and $ZnCl_2$ which have a porous morphology [6,7]. The advantage of Mg over other alloying elements can be described by its effectiveness even at low concentrations [8]. However, the addition of Mg reduces the adhesion of ZnMg coatings through the formation of brittle phases in the microstructure [9] and also due to the role of Mg on the reduction of "work of adhesion" [10].

Hot dip galvanization (HDG) and electrodeposition are common techniques to produce zinc coated steels. However, new challenges arise for the deposition of zinc coatings on advanced high strength steels (AHSS) using the conventional methods. Superficial segregation of the alloying elements (such as Mn, Cr and Si) in AHSS during annealing pretreatment leads to the surface oxidation before HDG and reduces the adhesion of zinc coatings [11]. High energy cost, environmental impacts and the possibility of hydrogen embrittlement can be stated as the main drawbacks of the electrodeposition process [12]. Physical vapor deposition (PVD) is considered as a possible breakthrough technology for continuous deposition of Zn alloys on an industrial scale. Low deposition temperature (~250 °C), large flexibility for the production of multilayered coatings with variable compositions, more accurate thickness control and environmental friendliness can be mentioned as the main advantages of the PVD process. A recent development concerns the feasibility of the production of the ZnMg coatings by the PVD process [13,14]. However, these types of coatings suffer from low adhesion to steel substrate and low formability. This signifies the importance of fundamental understanding of the role of process parameters and their impact on the formation of coating imperfections and ultimately to achieve a conclusive process window for the ZnMg PVD coatings.

Limited researches are published addressing the adhesion of ZnMg coatings. The adhesion behavior of single layer ZnMg coatings with different Mg content (deposited on steel substrate) was studied qualitatively by 180° bending and lap shear tests [9]. They found that the adhesion behavior of ZnMg coatings (in the low Mg content regime) depends mostly on the fraction of pure Zn phase, while the effect of coating thickness was negligible. The effect of insertion of an Al interlayer on the adhesion of ZnMg coatings was studied by Lee et al. [15] through the measurement of the delamination width in a scratch test. Metallic bonding was introduced as the main reason for obtaining excellent adhesion between Al and ZnMg. It was also found that the grain size of the ZnMg films decreases with increasing the Mg content. A semi-quantitative adhesion evaluation approach was introduced by La et al. [16] using a hybrid of punch stretching and potentio-dynamic polarization. It is reported that the microstructure of ZnMg coatings changes from a crystalline porous structure to a mixture of amorphous-nanocrystalline microstructure with increasing the Mg content that influences the adhesion properties.

So far, lack of profound understanding about the adhesion of ZnMg PVD coatings is sensible. The effect of thickness of the layers, Mg concentration and processing parameters on the adhesion strength are not fully understood yet. In other words, it is still not clear which parameters influence the overall adhesion performance of PVD ZnMg coated steels during the deformation. To obtain a thorough understanding of the adhesion behavior, ZnMg-Zn bilayer coatings with different Mg contents and also various thicknesses ratios are deposited on steel substrates and their adhesion performance are fundamentally investigated.

2. Materials and methods

Single layer ZnMg and bilayer ZnMg-Zn coatings with different combinations of Mg concentration (1.5–16.5 wt% Mg), thickness of Zn interlayer (0.2–2 μm) and thickness of the ZnMg top layer (3–6.8 μm) are deposited on two types of steel substrates: plain carbon steel (the so-called black plate steel) and a dual phase steel (DP800) by a thermal evaporation PVD process. Table 1 shows the chemical compositions of the steel substrates used in the present study. As the galvanizability of the steel substrates is different, both steels were selected for assessing the adhesion strength of vapor deposited ZnMg-Zn bilayer coatings.

The schematic of the deposition chamber is shown in Fig. 1. The chamber dimensions are 0.7 m in depth, 1.3 m in height, 2.85 m in length. The vacuum chamber of the setup is equipped with two crucibles containing molten Zn and ZnMg alloy, each of which is heated to the evaporation temperature. The generated vapor of the pure or the alloyed melt passes through a vapor distribution box (VDB) and is deposited on the running steel strip. The width of the steel strip is 300 mm and runs with a typical speed of 1–10 m/min. Prior to the deposition, the surface of the steel substrate is cleaned by magnetron sputtering with Ar^+ ions. The plasma cleaning removes the pre-existed oxide layers and preheats the substrate to a temperature of ~150 °C, depending on the plasma power. After the deposition of the Zn interlayer, the surface of Zn interlayer is again plasma cleaned to achieve a fresh interface for the deposition of the ZnMg top layer. The coatings are labeled as ZnMgX-Zn where X represents the Mg content in wt%. More information about the details of PVD process can be found in [17].

Grazing incidence X-Ray diffraction (Panalytical Xpert Pro MRD) is used for the phase analysis of the coatings. The microstructure of the coatings is investigated by scanning electron microscopy (Philips XL30-FEG ESEM) and transmission electron microscopy (JEOL 2010F), both equipped with an EDS detector. The cross section of the coatings is polished by a cryo cross-section polisher (JEOL IB-19520CCP) at −140 °C to avoid beam-induced defects. To measure the thickness of the coatings, three samples were sectioned randomly from each coated steels over the width of coated steel strip and the cross sections were carefully investigated. In-situ SEM tensile tests (Kammrath & Weiss 5000 N module) are performed to compare the mechanical properties of single layer ZnMg and bilayer ZnMg-Zn coatings. More information about the geometry of the in-situ tensile specimen and test setup are referred to [13].

The "adhesion performance" of the coating/substrate system is qualified by the standard bending based "BMW crash adhesion test" (BMW AA-M223) [17], while the ZnMg/Zn interfacial "adhesion strength" (in MPa) is quantified by the scratch test. The BMW crash adhesion test is a broadly accepted technique in industry to evaluate the adhesion of galvanized coatings. Initially, a line of an adhesive glue (Betamate 1496V DOW Automotive Systems) of 4–5 mm thickness is applied to the surface of the coating and heated at 175 °C for 30 min to cure the adhesive. After cooling, the samples are quickly bent over an angle of 90°. To pass the test, the samples should fail at the interface of the adhesive glue and the top surface of the coating [17].

Details of the scratch test parameters for the quantification of adhesion strength are shown in Table 2. The critical load (L_C) of the scratch test is defined as the load at which the first detectable delamination occurs at the ZnMg/Zn interface. The adhesion strength at the ZnMg/Zn interface is calculated using the developed Benjamin-Weaver model

Table 1
Chemical compositions (wt%) of the steel substrates.

Streel	C	Si	Mn	P	S	Ni	Cr	Cu	Fe
DP800	0.153	0.386	1.487	0.013	0.007	0.018	0.022	0.015	Bal.
Black plate	0.04–0.08	0.03	0.18–0.35	0.02	0.03	0.08	0.08	0.08	Bal.

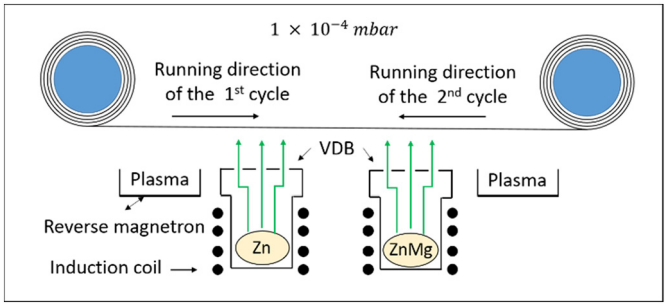

Fig. 1. Schematic of the deposition chamber of the PVD process to prepare ZnMg-Zn coatings.

recently published by the authors [13,14] as following:

$$F = \frac{K\, a\, H}{\sqrt{R^2 - a^2}} \tag{1}$$

where F is the adhesion strength (in MPa), K is a constant, R is the radius of indenter tip, H is considered as the hardness of substrate and "*a*" is the radius of contact circle at L_C as

$$a = \left(\frac{L_c}{\pi H}\right)^{0.5} \tag{2}$$

To consider the effect of both the steel and Zn interlayer as the substrate for ZnMg top layer, composite hardness is calculated using the defined weight factor as following [13,14]:

$$\omega = \frac{\text{Thickness of zinc interlayer}}{\text{Residual depth at } L_C} \tag{3}$$

$$H_{composite} = \omega\, H_{Zn} + (1-\omega)\, H_{steel} \tag{4}$$

Clear distinction should be made between the terms "adhesion performance" and "adhesion strength" in the whole article.

Finite element method (FEM) simulation is conducted to study the stress/strain distributions and failure behavior of PVD ZnMg-Zn bilayer coated steel during the BMW adhesion test. A set of simulations is executed on the bilayer coated steel with 6.8 μm thick ZnMg coating. The thicknesses of Zn coating and the steel substrate are considered as 1.7 μm and 200 μm, identical to the experimentally tested sample. The length of the simulated sample is 100 mm. The top epoxy glue adhered to the sheet is considered thick enough compared to the underlying specimen. The holder, die and the punch are set as rigid bodies while the sample comprised of the epoxy glue, Zn and ZnMg layers and the steel substrate is defined as homogenous deformable solids. Fig. 2 illustrates the geometry of the FEM model of the BMW adhesion test at different magnifications. The sample is completely fixed against rotations and displacements between the die and the holder. The punch presses the sheet up to 90° as far as the sample touches the die. The mechanical properties of each material are obtained by nanoindentation and tensile tests and employed in the model. The properties of the epoxy glue are derived from its technical datasheet. Ductile damage model is utilized to capture the failure/fracture behavior of the components. The simulation is performed in ABAQUS dynamic explicit 2D mode exploiting Arbitrary Lagrangian-Eulerian (ALE) mesh control. Mesh sensitivity of the results is resolved and an appropriate mesh refinement is performed, accordingly.

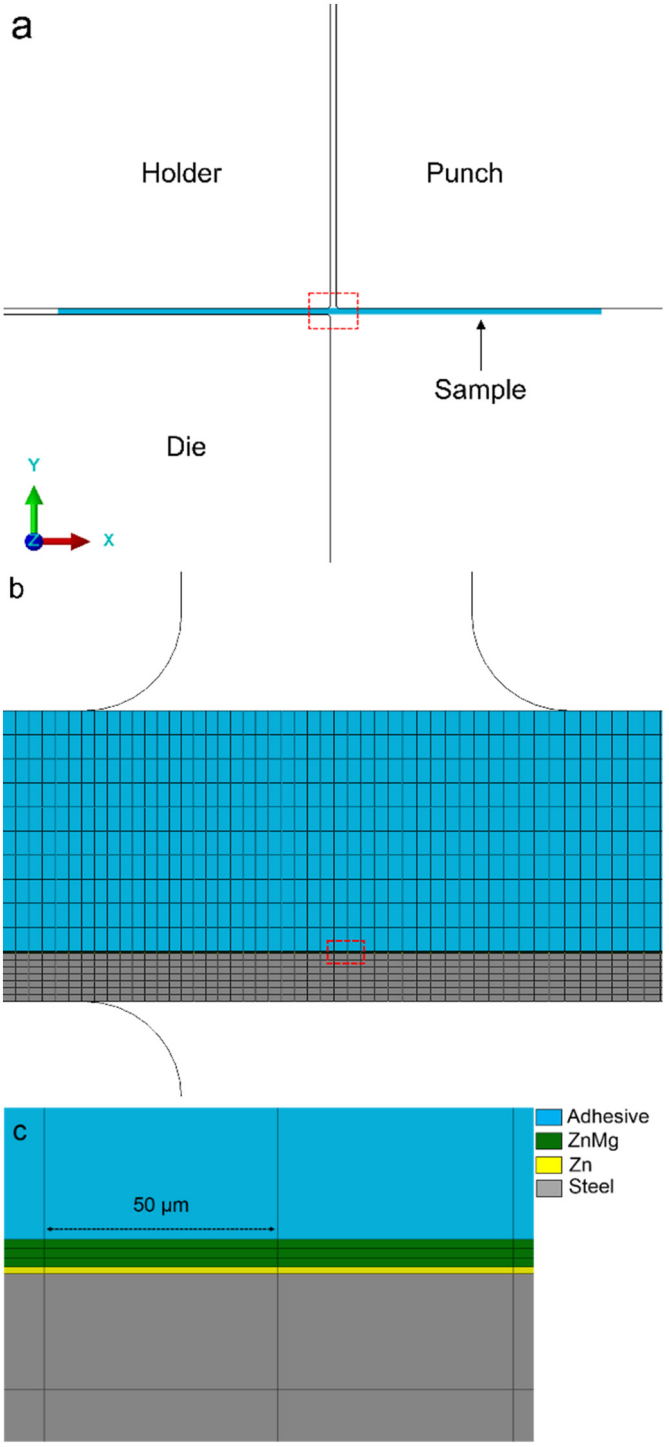

Fig. 2. Geometry of the finite element model of the BMW crash adhesion test at different magnifications: (a) overview, (b) elements structure and (c) detailed meshing over the ZnMg-Zn bi-layer coating.

Table 2
Parameters used in the scratch test for quantification of the interfacial adhesion strength.

Indenter type/material	Rockwell C/diamond
Radius of the indenter tip	200 μm
Maximum normal load	20 N for ZnMg-Zn coatings 50 N for the pure zinc coating
Loading rate	20 N/min for ZnMg-Zn coatings 50 N/min for the pure zinc coating
Scratch length	10 mm

3. Results and discussion

3.1. Theoretical calculation of the work of adhesion in ZnMg/Zn/steel system

The "work of adhesion" of a coating on a substrate is referred to the amount of work required to separate the coating from the substrate per unit of the interface area. For a coating composed of A and a substrate composed of B, the work of adhesion can be estimated using the "Macroscopic atom" model as following [18]:

$$W_{ad} = \gamma_A^S + \gamma_B^S - \gamma_{A-B}^I \tag{5}$$

where γ_A^S and γ_B^S are the surface energies of A and B, respectively, and γ_{A-B}^I is the interface energy between A and B.

Assuming that the coating and the substrate are solid solutions of a mixture of m number and n number elements, respectively, the Eqs. (6)–(7) can be used to describe the surface energies for the solid solutions A and B [19].

$$\gamma_{A_1 \ldots A_m}^S = \sum_{i=1}^{m} C_{A_i}^S \gamma_{A_i}^S - \sum_{i=1}^{m-1} \sum_{j=i+1}^{m} C_{A_i}^S C_{A_j}^S \frac{\Delta H_{A_i \text{ in } A_j}^I}{C_0 V_{A_i}^{\frac{2}{3}}} \tag{6}$$

$$\gamma_{B_1 \ldots B_n}^S = \sum_{i=1}^{n} C_{B_i}^S \gamma_{B_i}^S - \sum_{i=1}^{n-1} \sum_{j=i+1}^{n} C_{B_i}^S C_{B_j}^S \frac{\Delta H_{B_i \text{ in } B_j}^I}{C_0 V_{B_i}^{\frac{2}{3}}} \tag{7}$$

where $C_{A_i}^S$ and $C_{A_j}^S$ are the surface fractions of A_i and A_j elements. $C_{B_i}^S$ and $C_{B_j}^S$ are also the surface fractions of B_i and B_j elements. $\Delta H_{A_i \text{ in } A_j}^I$ is the enthalpy change for solution of 1 mol A_i in an infinite amount of A_j. Similarly, $\Delta H_{B_i \text{ in } B_j}^I$ is the enthalpy change for solution of 1 mol B_i in an infinite amount of B_j. C_0 is a constant relating the atomic volume to the atomic surface area in the unit cell.

The surface fraction of element A_i ($C_{A_i}^S$) and the surface fraction of element B_i ($C_{B_i}^S$) are calculated by the following equations [18]:

$$C_{A_i}^S = \frac{C_{A_i} V_{A_i}^{\frac{2}{3}}}{\sum_{i=1}^{n} C_{A_i} V_{A_i}^{\frac{2}{3}}} \tag{8}$$

$$C_{B_i}^S = \frac{C_{B_i} V_{B_i}^{\frac{2}{3}}}{\sum_{i=1}^{n} C_{B_i} V_{B_i}^{\frac{2}{3}}} \tag{9}$$

The interface energy between coating A and substrate B is a sum of two components [19]:

$$\gamma_{A-B}^I = \gamma_{A-B}^{mismatch} + \gamma_{A-B}^{interaction} \tag{10}$$

$\gamma_{A-B}^{mismatch}$ is related to the strain energy due to the mismatch between A and B at their interface while $\gamma_{A-B}^{interaction}$ is related to the chemical interaction of the elements in different phases. Assuming the interface is a high angle grain boundary [10], the mismatch energy can be approximated by [18]:

$$\gamma_{A-B}^{mismatch} = \frac{1}{6}\left(\gamma_{A_{1,\ldots,m}}^S + \gamma_{B_{1,\ldots,n}}^S\right) \tag{11}$$

Considering the role of all elements at the interface, the total contribution of chemical interaction in γ_{A-B}^I can be calculated as [19]:

Table 3
The calculated work of adhesion for different interfaces.

Type of interface	DP800/Zn	Black plate/Zn	Zn/Mg_2Zn_{11}	$Zn/MgZn_2$
Work of adhesion (J/m^2)	2.98	3.06	1.62	1.6

$$\gamma_{A_{1,\ldots,m}-B_{1,\ldots,n}}^{Interaction} = \sum_{i=1}^{m} \sum_{j=1}^{n} C_{A_i}^S C_{B_j}^S \frac{\Delta H_{A_i \text{ in } B_j}^I}{C_0 V_{A_i}^{\frac{2}{3}}} \tag{12}$$

Table 3 shows the result of the calculated work of adhesion of DP800/Zn, black plate steel/Zn, Zn/Mg_2Zn_{11} and $Zn/MgZn_2$ interfaces. It is noteworthy that the reported values are the outcome of the theoritical model presented above which only considers the thermodynamic properties of the materials, not their physical and mechanical properties. The work of adhesion at the black plate steel/Zn interface is a bit higher than that of the DP800/Zn. The reason for the lower work of adhesion at DP800/Zn interface is due to the higher content of some alloying elements such as Si and Mn in DP800 compared to that in the black plate steel [10]. Nontheless, the calculated work of adhesion between the steel substrates and Zn is notably higher than that of the Mg_2Zn_{11}/Zn and $MgZn_2$/Zn interfaces. It reveals that, in a ZnMg-Zn bilayer coated steel, the interface between the ZnMg top layer and the Zn interlayer is inherently weaker than the steel/Zn interface. The calculated "work of adhesion" are in good agreement with the experimental results published in [13], where, during the scratch test, the ZnMg top layer starts to delaminate from the Zn interlayer prior to the final failure at the steel/Zn interface.

3.2. Microstructural studies

Fig. 3 shows the XRD patterns of ZnMg top layer as a function of Mg concentration. It is found that the ZnMg top layer consists of a mixture of Zn and Mg_2Zn_{11} phases at the Mg concentrations <~5 wt%. The microstructure of the ZnMg top layer is fully covered by a mixture of Mg_2Zn_{11} and $MgZn_2$ intermetallic phases at higher Mg concentrations and turns into $MgZn_2$ single phase at the Mg concentration of ~14 wt%. Some unreacted pure Zn and Mg are also found along with $MgZn_2$ at higher Mg concentrations (16.5 wt% Mg). Higher Mg content in the molten alloy may lead to the saturation of vapor by magnesium atoms. The desublimation time in the PVD process seems not long enough to promote a complete reaction between Zn and Mg atoms. Therefore, some unreacted pure elements remain in the microstructure. It is worth noting that broadening of the $MgZn_2$ peaks as well as their reduced intensity at such high Mg concentration indicates that the structure of $MgZn_2$ is transformed to an amorphous/nanocrystalline state.

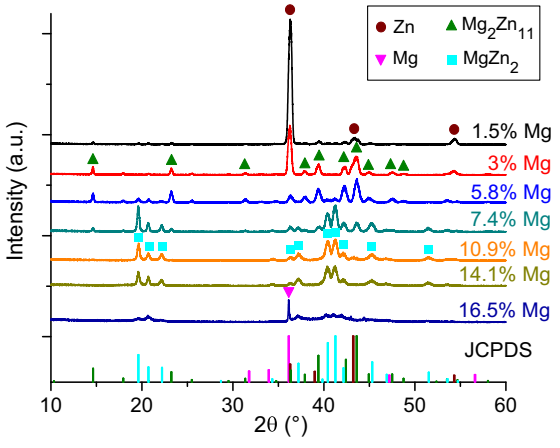

Fig. 3. XRD patterns of the ZnMg coatings with different Mg concentrations.

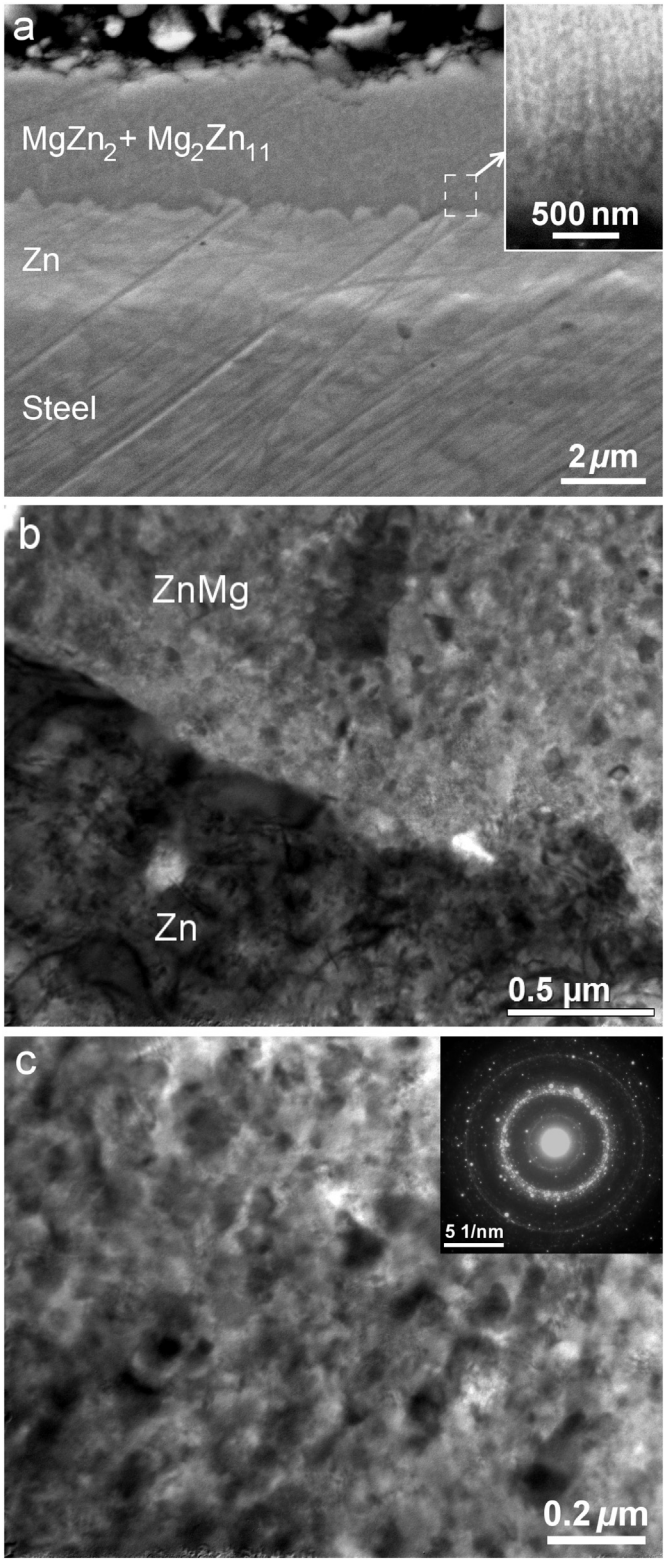

Fig. 4. Microstructure of ZnMg11-Zn bilayer coating: (a) cross section SEM micrograph, (b) cross section TEM micrograph of the interface of ZnMg/Zn, (c) cross section TEM micrograph of ZnMg top layer and its selected area diffraction pattern.

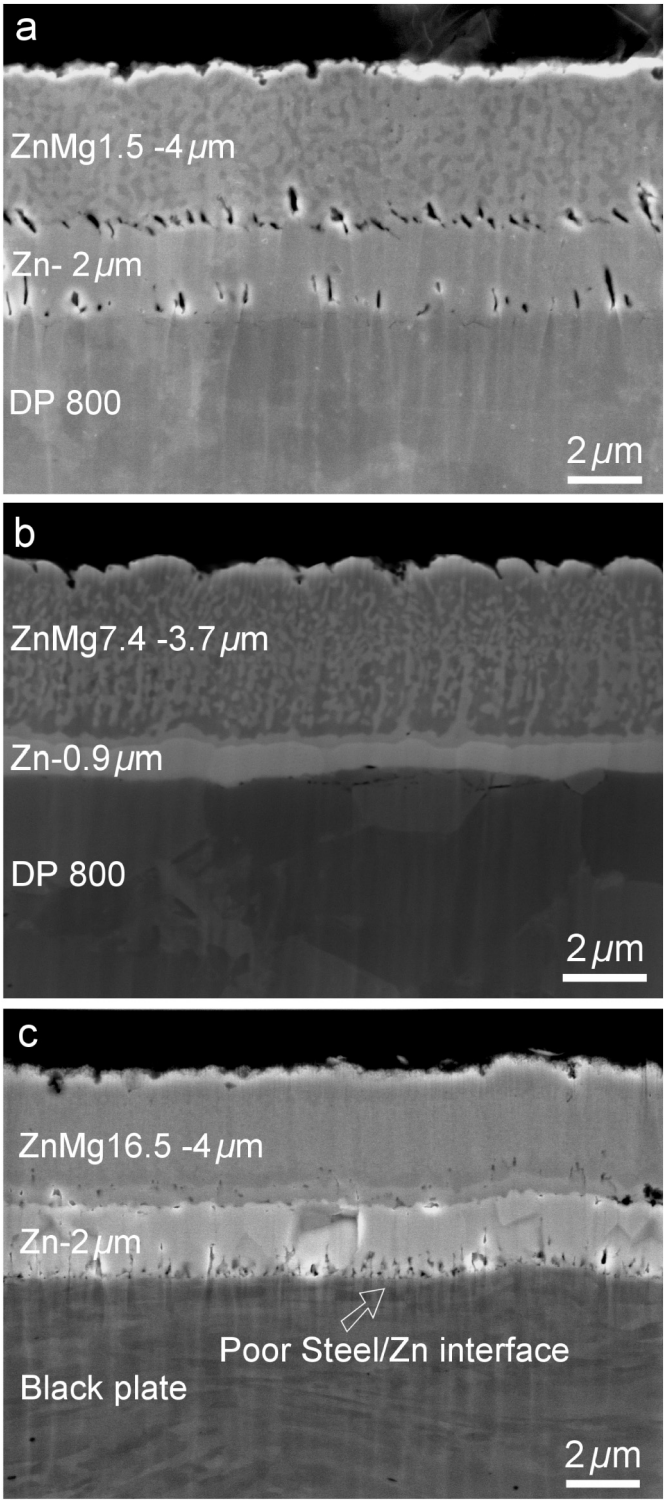

Fig. 5. Typical examples of the cross section of the ZnMg-Zn bi-layered coatings: (a) ZnMg1.5-Zn, (b) ZnMg7.4-Zn and (c) ZnMg16.5-Zn.

It has been found out that the ZnMg coatings with higher Mg concentrations show enhanced corrosion resistance [16]. Therefore, a bi-layer coating containing 11 wt% Mg is selected as a representative for detailed microstructural investigation. Fig. 4 shows the cross sectional SEM and TEM micrographs of ZnMg11-Zn bilayer coating in the as-deposited condition. The ZnMg layer is a mixture of finely distributed nanocrystalline $MgZn_2$ and Mg_2Zn_{11} intermetallic compounds (Fig. 4a–b). The selected area diffraction (Fig. 4c inset) reveals that both phases are in nanocrystalline state and no sign of amorphous phase is found in the microstructure. The EDS analysis confirms that a thin layer of Mg_2Zn_{11} (consisting 91.74 wt% Zn and 8.26 wt% Mg) with an average thickness of 200 nm is present at the interface of

ZnMg/Zn. This implies that the growth of ZnMg at the interface during the deposition starts with the formation of Mg_2Zn_{11} layer followed by simultaneous nucleation and growth of $MgZn_2$ and Mg_2Zn_{11} phases. This finding is in good agreement with the Zn-Mg binary phase diagram that the interface of $MgZn_2$ and pure Zn is not thermodynamically stable. Therefore, the formation of Mg_2Zn_{11} as an intermediate layer between the top layer and Zn is inevitable.

Fig. 5 shows the typical cross sectional SEM micrographs of the prepared coatings. Some interfacial defects are found at the Zn/steel and/or ZnMg/Zn interfaces in some coatings. Based on the position of the interfacial defects, the coatings are divided into three categories: coatings having interfacial defects at both Zn/steel and ZnMg/Zn interfaces (Fig. 5a), coatings without any defect at the interfaces (Fig. 5b) and coatings with some defects in one of the interfaces (Fig. 5c). However, as PVD process is under development as a breakthrough technology for continuous deposition of ZnMg-Zn bilayer coatings on the advanced and/or ultra high strength steels on an industrial scale, the nature of the presence of some process-related defects in the coating is still under investigation. Based on the observations, defect formation is not influenced by the thickness and the chemical composition of the layers while it is speculated that the pre-treatment of the surface of steel substrate and Zn interlayer as well as the deposition process parameters govern the formation of the voids.

3.3. Single layer ZnMg versus bilayer ZnMg-Zn coatings

Experimental results indicate that single layer ZnMg coatings always show inferior adhesion to the steel subtrate and usually fail the BMW adhesion test in contrast to the ZnMg-Zn bi-layer coatings [13]. To show the difference more clearly, in-situ tensile tests are carried out on both the ZnMg single layer and the ZnMg-Zn bilayer coatings (Figs. 6 and 7). It is worthy to mention that the maximum strain that can be applied to the coating is limited by the elongation limit of the underlying steel substrate. It means that the maximum deformation of the coating occurs in the vicinity of the fractured area of steel substrate in uniaxial tensile test. Fig. 6 shows the SEM micrographs of the single layer ZnMg after the tensile test. As seen, large areas of the coating (in the ranges of mm) are chipped off from the steel substrate at the rupture point. It implies that the adhesion of the single layer ZnMg coating to the steel substrate is low to resist the shear stress at the interface. On the other hand, in the case of the ZnMg-Zn bilayer coating, both the ZnMg top layer and the Zn interlayer are still adhered to the steel substrate after the tensile test (Fig. 7). It means that the addition of a ductile Zn interlayer between the steel substrate and the ZnMg top layer can accommodate a large portion of the interfacial shear stress. This is evident by the partially pull out of the Zn interlayer from/underneath the edges of the coating segments at the failed region (see Fig. 7b). It confirms that the presence of Zn interlayer is essential for obtaining a good adhesion in ZnMg coated steels.

3.4. Quantification of the adhesion strength

3.4.1. The effect of the thickness of Zn interlayer on the adhesion

The adhesion strength of the coatings at the ZnMg/Zn interface is quantified by the scratch test. Primarily, three coatings with similar ZnMg top layer (6.5 wt% Mg and ~3 μm thick) and different thicknesses of the Zn interlayer (0.2 μm, 0.7 μm and 1.3 μm) are characterized to study the effect of the thickness of Zn interlayer (t_{Zn}) on the interfacial adhesion strength and also the adhesion performance in the BMW adhesion test (Table 4). The results of the scratch test reveal that, although the critical load of delamination increases with increasing the thickness of the interlayer, the interfacial adhesion strength at the ZnMg/Zn interface is closely equal for the three investigated samples (~110 MPa). This indicates that the interfacial adhesion strength at the ZnMg/Zn interface

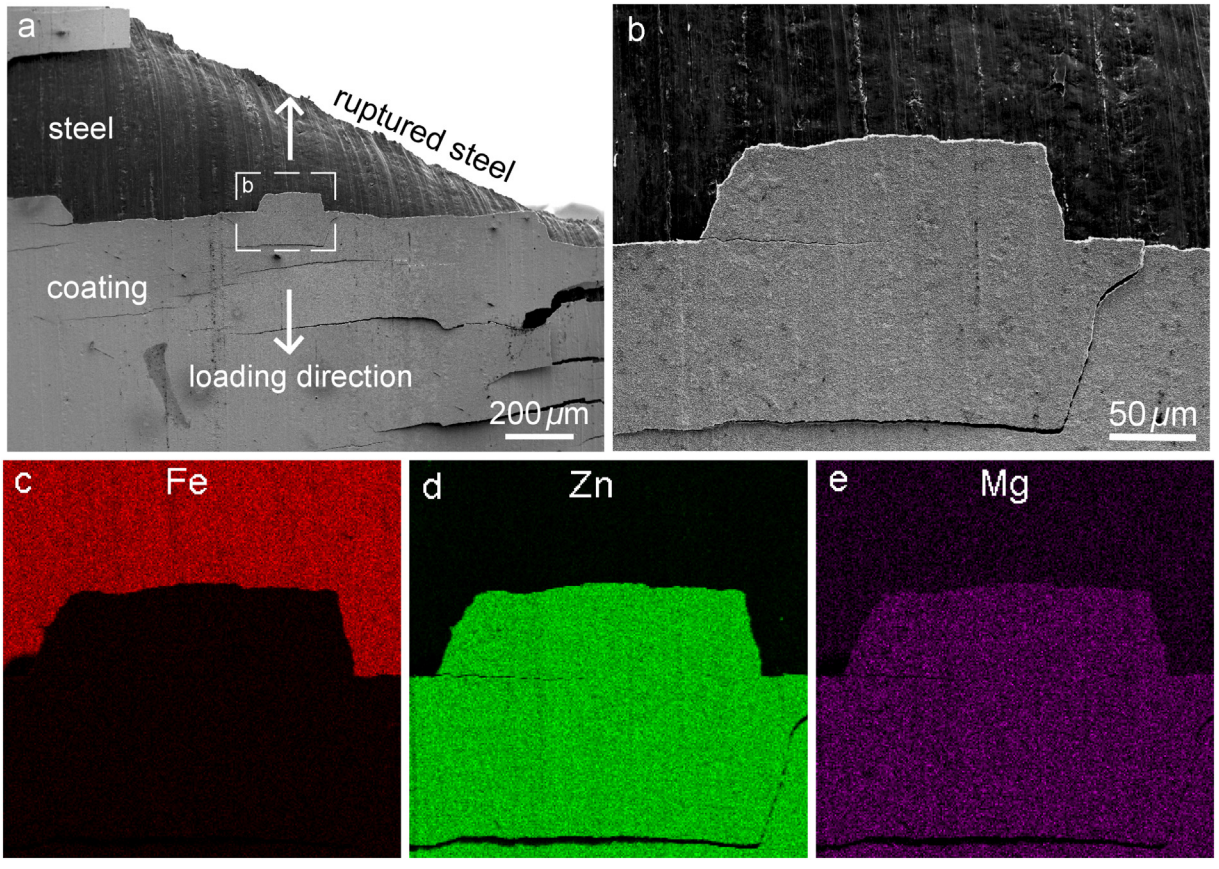

Fig. 6. SEM micrographs of the single layer ZnMg coated steel after the tensile test along with the EDS elemental mapping of (b).

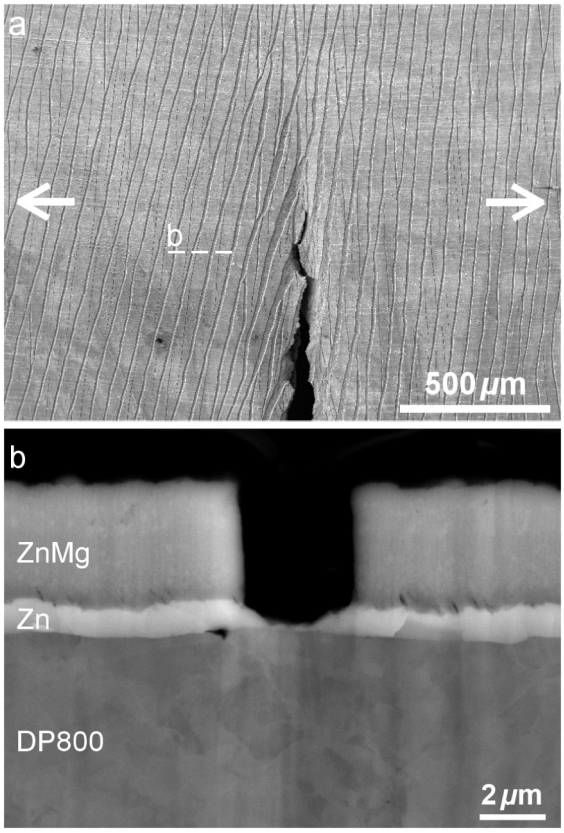

Fig. 7. SEM micrographs of the ZnMg7.4-Zn bi-layered coatings after the tensile test with two arrows indicating the loading direction: (a) overal view, (b) cross sectional view of a crack after unloading.

is independent of t_{Zn}. Although the interfacial adhesion strength is almost equal for the three investigated coatings, the coating with the thinnest t_{Zn} fails in the BMW crash adhesion test, while the others pass. This behavior can be attributed to the role of the ductile zinc interlayer in accommodating the shear stress/strain during bending. It has been already observed in our previous study [14] that failure in BMW crash adhesion test occurs when t_{Zn} is smaller than a threshold ($t_{Zn}^{Min} \cong$ 500 nm). Therefore, the adhesion performance of a bilayer coating/substrate system during bending does not only depend on the interfacial adhesion strength, but also on the structure parameters such as t_{Zn}.

3.4.2. The effect of process-induced defects on the adhesion

The adhesion strength of the bilayer coatings at the ZnMg/Zn interface versus Mg concentration for different levels of defect density is shown in Fig. 8. It is worth to mention that the thickness of the ZnMg top layer for the investigated coatings in Fig. 8 is limited to about 3–4 μm. The pure zinc coating has the highest adhesion strength (171 MPa) among the other samples. For the defect-free coatings, the interfacial adhesion strength (σ) at the ZnMg/Zn interface reduces gradually with increasing the Mg content of the top layer and eventually reaches to 66 MPa at 16.5 wt% Mg. The exponential relation (Eq. (13)) follows the experimental data with a high coefficient of determination ($R^2 = 0.977$). This relation is marked by the green line in Fig. 8:

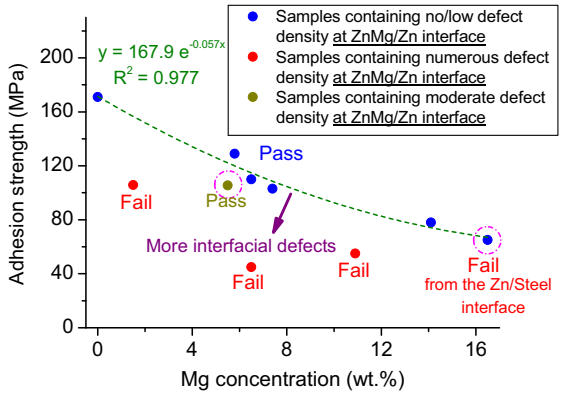

Fig. 8. Adhesion strength of the bi-layered coatings at the ZnMg-Zn interface versus the Mg content.

$$\sigma = 167.9 \ exp^{-0.057 \times C_{Mg}} \quad (13)$$

where C_{Mg} is the Mg content of the ZnMg top layer in wt%. The adhesion strength of all of the coatings having interfacial defects falls below the fitted curve of adhesion strength of the defect-free coatings. Higher defects density at the ZnMg/Zn interface results in an even larger drop in the adhesion strength compared to the defect-free coating. For instance, the adhesion strength of the ZnMg5.5-Zn coating with a moderate amount of interfacial defects is ~105 MPa, slightly lower than the defect-free sample. This coating can still pass the BMW adhesion test. In contrast, the ZnMg1.5-Zn coating containing a high density of defects and with the same magnitude of the interfacial adhesion strength (105 MPa) fails in the BMW adhesion test because it is relatively far from the fitted curve. In other words, at a given Mg content, the density of the interfacial defects determines how far the adhesion strength deviates from that of the ideal coating. This indicates that the density of the interfacial defects can also influence the adhesion performance in the BMW adhesion test.

3.4.3. The effect of the thickness of ZnMg top layer on the adhesion

As shown earlier, the ZnMg-Zn bilayer coatings with t_{Zn} larger than t_{Zn}^{Min} can pass the BMW adhesion test in the absence of interfacial defects or containing low density of interfacial defects. However, further study with a thicker ZnMg top layer reveals that to fulfill the BMW adhesion test, there exists also a maximum thickness for the ZnMg top layer ($t_{ZnMg}^{Max} \cong$ 3.5 μm) that might be a function of the thickness of the Zn interlayer. t_{ZnMg}^{Max} varies slightly with the Mg content of the top layer. Table 5 presents the mechanical properties of the ZnMg top layer measured by nanoindentation. As can be seen, the hardness and the elastic modulus of the ZnMg top layer increases with the increase in Mg content up to ~7.4 wt% and reach to constant values at higher concentrations. The ratio of $\frac{H^3}{E^2}$ expresses the resistance of a material to plastic deformation

Table 4
Summary of the effect of the thickness of Zn interlayer (t_{Zn}) on the adhesion of ZnMg-Zn bi-layered coatings.

	t_{Zn} (μm)	t_{ZnMg} (μm)	Critical load of delamination (N)	Adhesion strength (MPa)	Results of BMW adhesion test
ZnMg6.5-Zn[a]	0.2	3	11.6 ± 0.4	108 ± 1.8	Fail
ZnMg6.5-Zn[a]	0.7	3	13.1 ± 0.5	111 ± 2.5	Pass
ZnMg6.5-Zn[a]	1.3	3.1	13.3 ± 0.2	105 ± 1.2	Pass

[a] The thickness of the Zn interlayer is different for these samples.

Table 5
Mechanical properties of the ZnMg top layer of the samples containing different Mg content.

	Hardness (GPa)	Elastic modulus (GPa)	$\frac{H^3}{E^2}$ (GPa)
ZnMg1.5	1.02 ± 0.35	66 ± 14.4	0.00024
ZnMg5.8	3.18 ± 0.80	90 ± 14.3	0.00397
ZnMg7.4	4.97 ± 1.10	104 ± 16.0	0.01135
ZnMg10.9	5.15 ± 1.05	103 ± 15.8	0.01300
ZnMg14.1	5.30 ± 1.40	103 ± 17.5	0.01387

[20,21]. Higher Mg contents results in a less ductility. Therefore, t_{ZnMg}^{Max} can be slightly lower for the coatings with higher Mg contents.

Fig. 9a shows the cross section of the ZnMg14.5-Zn coating with a 6.8 μm thick top layer which has failed in the BMW adhesion test. The SEM micrographs of the exposed side of the coating remained on the substrate after the failure, are shown in Fig. 9b–c. The results of the EDS analysis of different areas on the failed surface are shown in Table 6. Although the content of Mg varies from area to area due to the different thickness of remaining ZnMg top layer after fracture, it can be concluded that the failure of bilayer coatings with a top layer thicker than t_{ZnMg}^{Max} occurs in the form of a cohesive brittle fracture across the ZnMg top layer. This behavior can be related to the brittleness of $MgZn_2$ intermetallic phase as stated before.

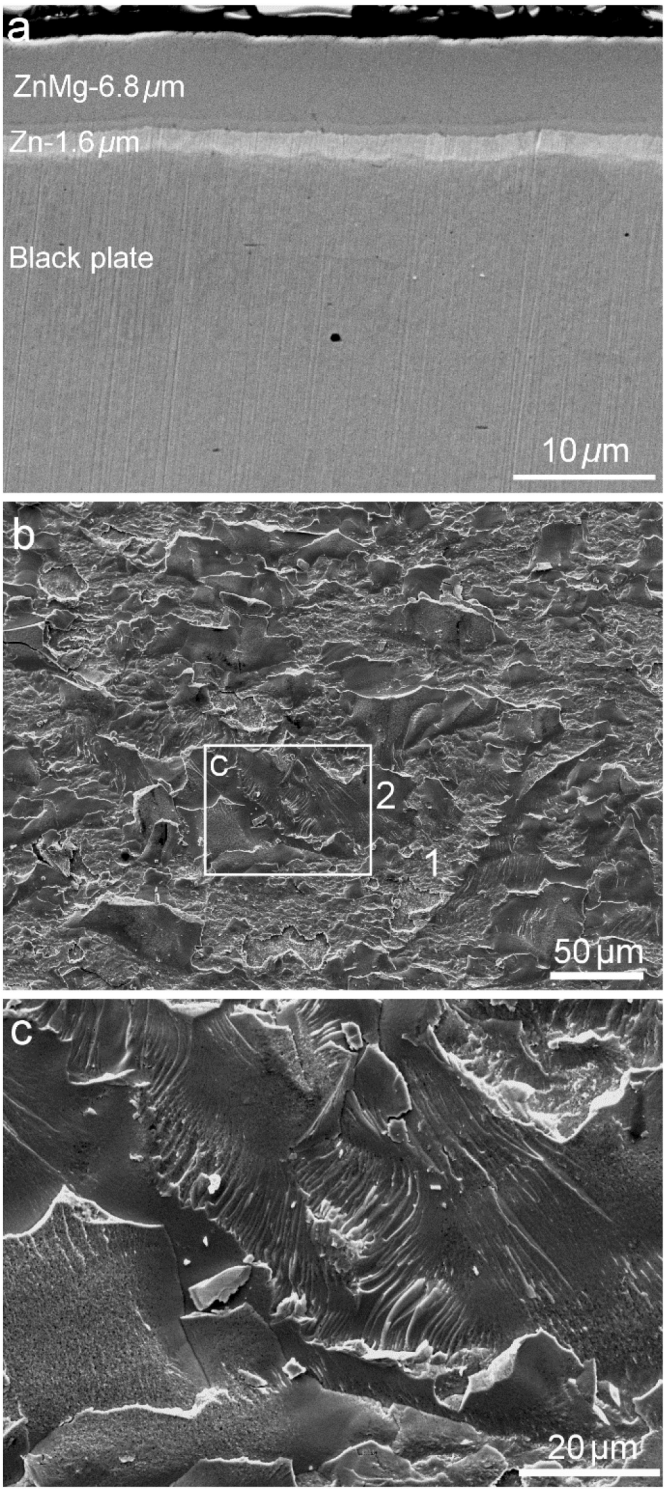

Fig. 9. (a) Cross section SEM micrograph of the ZnMg14.5-Zn coating with a 6.8 μm thick ZnMg, (b–c) SEM micrographs of the exposed side of the coating remained on the substrate after failure in the BMW adhesion test.

Table 6
Chemical composition of different points in Fig. 9b.

Location	Zn content (wt%)	Mg content (wt%)
Spot 1	95.44	4.56
Spot 2	84.72	15.27

Fig. 10 demonstrates the FEM simulation results to capture the failure mechanism in the ZnMg-Zn bilayer coated steel during the BMW adhesion test. It has to be pointed out that the thicknesses and the mechanical properties of the simulated coating are considered the same as the experimentally studied sample in Fig. 9a. Furthermore, a defect-free interface has been considered for the simulation. As shown in Fig. 10a, the top layer epoxy starts to fracture around 45° bending angle. Further failure of the epoxy is severely increased by increasing the bending angle due to the larger deformation until the bending angle of 90°. Fig. 10b shows the sample at the end of the simulation. As it can be noticed, the epoxy adhesive is severely damaged and failed in the vicinity of the ZnMg top layer. Equivalent plastic strain distribution of the magnified region associated with the ZnMg-Zn coatings and steel substrate is given in Fig. 10c. As it can be observed, most of the strain generated in the system is carried by the Zn interlayer due to its higher ductility compared to the ZnMg layer. The Zn interlayer seems to have endured the shear plastic deformation throughout the BMW adhesion test. On the other hand, the brittle ZnMg layer has failed in some regions. According to the stress distribution contour (Fig. 10d), the bottom area of the ZnMg coating adhered to Zn interlayer has experienced a higher stress magnitude and failed, consequently. Therefore, the FEM simulation results confirm that ZnMg coating has undergone cohesive failure as a result of internal stress concentration generated by severe plastic deformation during the BMW adhesion test.

3.4.4. Interdependency of the process parameters

The thickness of the ZnMg layer is mainly controlled by the evaporation temperature (vapor pressure), the travelling speed of the strip and also the design of the VDB. As an example, the effect of the evaporation temperature (at a constant travelling speed of 2 m/min) on the thickness of ZnMg14.5 layer is shown in Fig. 11a. The thickness of the ZnMg layer is reduced from 6.8 μm to 1.3 μm with the decrease in the evaporation temperature from 725 °C to 660 °C. However, decreasing the evaporation temperature to less than 700 °C causes a defective interface between the ZnMg and Zn layers, resulting failure in the BMW adhesion test (Fig. 11b–c). Therefore, to obtain a proper interface between the ZnMg and Zn layer and also to keep the thickness in a desirable range (~3.5 μm), the evaporation temperature has to be kept above 700 °C and the strip travelling speed should be increased, accordingly (Fig. 12d).

As a summary, it can be concluded that the adhesion performance of the ZnMg-Zn bilayer coating during the bending test is a complex function of different parameters such as the thickness of Zn and ZnMg layers, interfacial adhesion strength and the interfacial defect density as schematically depicted in Fig. 12. For industrial applications, it should be pointed out that although lower Mg concentration may lead to a higher interfacial adhesion strength, it degrades the superior corrosion resistance of ZnMg coatings which is achieved at higher Mg contents. Therefore, within a desirable window for the Mg content, the thickness of the layers should be kept in a range that yields the highest mechanical performance as well as economic justification. The appropriate thickness range for the Zn intermediate layer and the ZnMg top layer is 1–2 μm and 2–3.5 μm, respectively. Thickness control can be engineered by

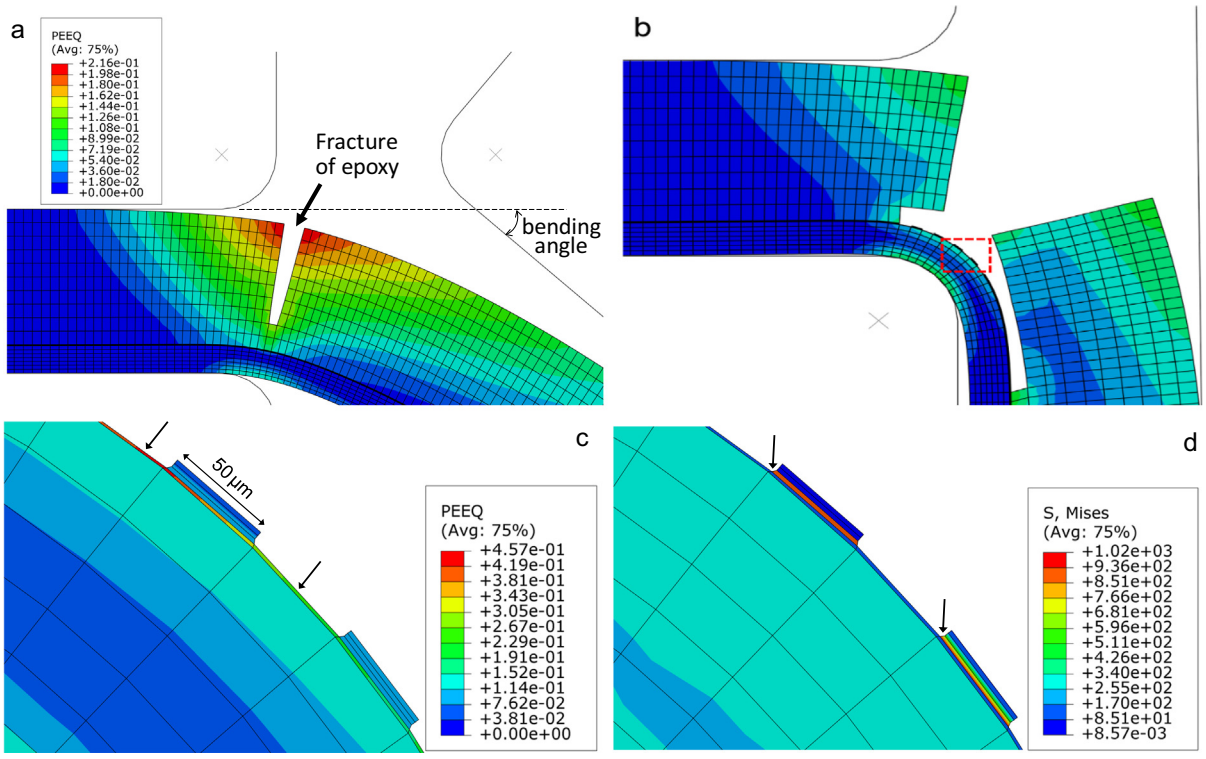

Fig. 10. Finite element simulation of the ZnMg-Zn bi-layered coating in BMW crash adhesion test; (a) failure of the adhesive glue at a bending angle of ~45°, (b) overview of the sample at the end of the simulation, (c) equivalent plastic strain and (d) Von misses stress at the bending angle of 90°.

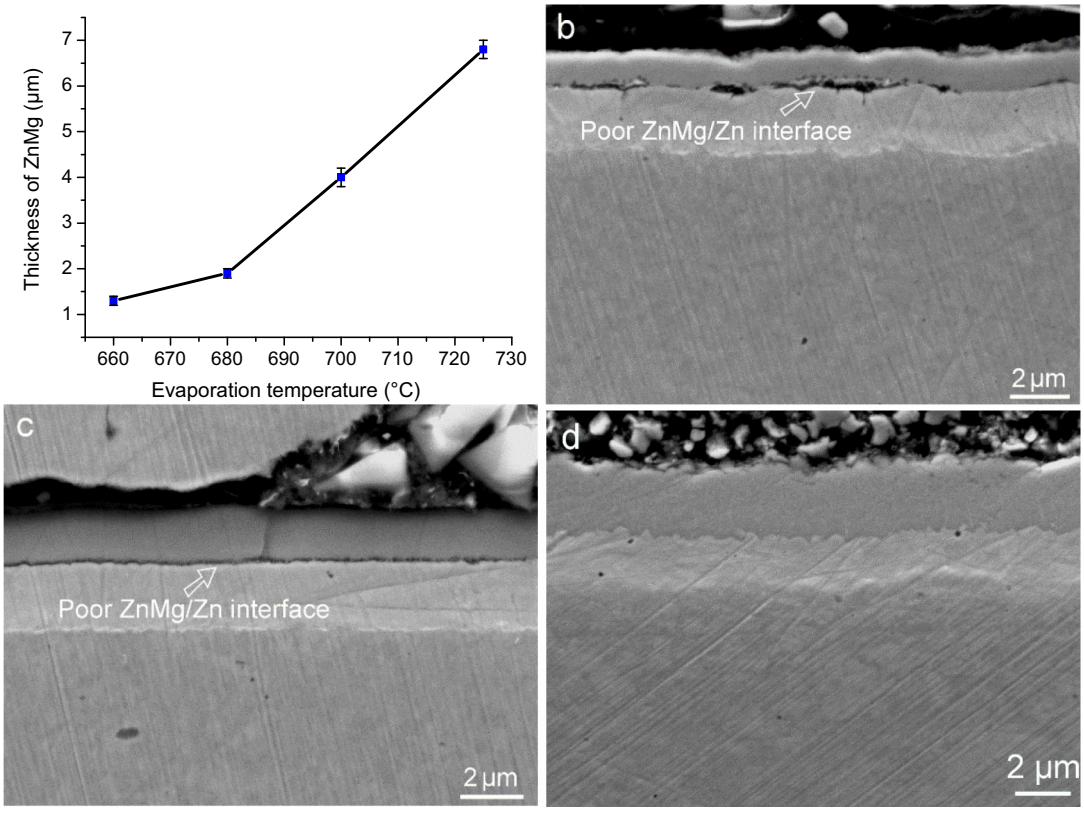

Fig. 11. (a) The effect of the evaporation temperature on the thickness of ZnMg14.5-Zn layer; cross section SEM micrographs showing the interface of ZnMg and Zn layers formed at the evaporation temperatures of (b) 660 °C, (c) 680 °C and (d) 725 °C.

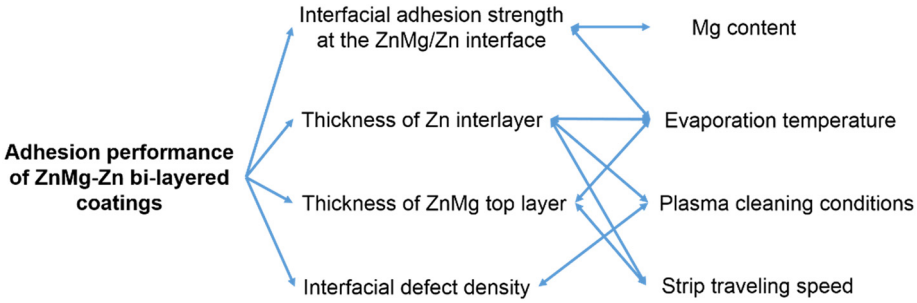

Fig. 12. Governing parameters for the adhesion performance of ZnMg-Zn bi-layered coatings in the BMW crash adhesion test.

variation of the evaporation temperature, strip travelling speed as well as plasma cleaning parameters.

4. Conclusions

The present investigation studies the fundamentals of adhesion of physical vapor deposited ZnMg coatings. The most important findings are as the following:

- Addition of Zn interlayer is essential for a sound adhesion performance for the ZnMg coatings.
- Theoretical calculations show that the work of adhesion at the ZnMg/Zn interface (~1.6 J/m^2) is notably lower than that of the steel/Zn interface (~3 J/m^2). This implies that the interface of ZnMg/Zn is inherently weaker than that of steel/Zn.
- Adhesion strength at the interface of ZnMg/Zn can be successfully quantified by the scratch test. The interfacial adhesion strength at the ZnMg/Zn interface depends mostly on the Mg content of the top layer and the density of interfacial defects. It is also found that the thickness of the zinc interlayer does not play a role in the interfacial adhesion strength.
- The adhesion performance of the ZnMg-Zn bilayer coatings in the BMW adhesion test is not only a function of the interfacial adhesion strength, but also the thickness of Zn and ZnMg layers as well as the density of the interfacial defects.
- There is a threshold value ($t_{ZnMg}^{Max} \cong 3.5$ μm) for the thickness of ZnMg layer beyond which the coating fails in the BMW adhesion test by cohesive brittle fracture.

CRediT authorship contribution statement

S. Sabooni: Conceptualization, Data curation, Investigation, Methodology, Writing - original draft. **M. Ahmadi:** Data curation, Validation. **E. Galinmoghaddam:** Data curation, Investigation, Writing - original draft. **R.J. Westerwaal:** Investigation, Writing - review & editing. **C. Boelsma:** Writing - review & editing. **E. Zoestbergen:** Writing - review & editing. **G.M. Song:** Investigation, Methodology. **Y.T. Pei:** Funding acquisition, Conceptualization, Methodology, Formal analysis, Writing - original draft, Supervision.

Declaration of competing interest

The authors declare that they have no known competing financial interests or personal relationships that could have appeared to influence the work reported in this paper.

Acknowledgement

This research was carried out under project number 13942 (S22.3.13513a) in the framework of the Partnership Program of the Materials innovation institute M2i (www.m2i.nl) and the Technology Foundation STW (www.stw.nl), which is part of the Netherlands Organisation for Scientific Research (www.nwo.nl).

References

[1] V. Kuklík, J. Kudláček, Hot-dip Galvanizing of Steel Structures, Butterworth-Heinemann, 2016.
[2] S. Rashmi, L. Elias, A.C. Hegde, Multilayered Zn-Ni alloy coatings for better corrosion protection of mild steel, Eng. Sci. Technol. Int. J. 20 (2017) 1227–1232.
[3] Y. Wang, J. Zeng, Effects of Mn addition on the microstructure and indentation creep behavior of the hot dip Zn coating, Mater. Des. 69 (2015) 64–69.
[4] N. LeBozec, D. Thierry, D. Persson, J. Stoulil, Atmospheric corrosion of zinc-aluminum alloyed coated steel in depleted carbon dioxide environments, J. Electrochem. Soc. 165 (2018) C343–C353.
[5] C. Yao, Z. Wang, S.L. Tay, T. Zhu, W. Gao, Effects of Mg on microstructure and corrosion properties of Zn–Mg alloy, J. Alloys Compd. 602 (2014) 101–107.
[6] E. Diler, B. Lescop, S. Rioual, G. Nguyen Vien, D. Thierry, B. Rouvellou, Initial formation of corrosion products on pure zinc and $MgZn_2$ examinated by XPS, Corr. Sci. 79 (2014) 83–88.
[7] E. Diler, S. Rioual, B. Lescop, D. Thierry, B. Rouvellou, Chemistry of corrosion products of Zn and MgZn pure phases under atmospheric conditions, Corr. Sci. 65 (2012) 178–186.
[8] M.S. Oh, S.H. Kim, J.S. Kim, J.W. Lee, J.H. Shon, Y.S. Jin, Surface and cut-edge corrosion behavior of Zn-Mg-Al alloy-coated steel sheets as a function of the alloy coating microstructure, Met. Mater. Int. 22 (2016) 26–33.
[9] W.S. Jung, C.W. Lee, T.Y. Kim, B.C. De Cooman, Mg content dependence of EML-PVD Zn-Mg coating adhesion on steel strip, Metall. Mater. Trans. A 47 (2016) 4594–4605.
[10] G.M. Song, W.G. Sloof, Effect of alloying element segregation on the work of adhesion of metallic coating on metallic substrate: application to zinc coatings on steel substrates, Surf. Coat. Technol. 205 (2011) 4632–4639.
[11] F. Li, H. Liu, W. Shi, R. Liu, L. Li, Hot dip galvanizing behavior of advanced high strength steel, Mater. Corros. 63 (2012) 396–400.
[12] E.M.K. Hillier, M.J. Robinson, Hydrogen embrittlement of high strength steel electroplated with zinc–cobalt alloys, Corros. Sci. 46 (2004) 715–727.
[13] S. Sabooni, E. Galinmoghaddam, M. Ahmadi, R.J. Westerwaal, J. van de Langkruis, E. Zoestbergen, J.Th.M. De Hosson, Y.T. Pei, Microstructure and adhesion strength quantification of PVD bi-layered ZnMg-Zn coatings on DP800 steel, Surf. Coat. Technol. 359 (2019) 227–238.
[14] S. Sabooni, E. Galinmoghaddam, H.T. Cao, R.J. Westerwaal, E. Zoestbergen, J.Th.M. De Hosson, Y.T. Pei, New insight into the loss of adhesion of ZnMg-Zn bi-layered coatings, Surf. Coat. Technol. 370 (2019) 35–43.
[15] M. Lee, I. Bae, Y. Kwak, K. Moon, Effect of interlayer insertion on adhesion properties of ZnMg thin films on steel substrate by PVD method, Curr. Appl. Phys. 12 (2012) S2–S6.
[16] J.H. La, K.T. Bae, S.Y. Lee, K.H. Nam, A hybrid test method to evaluate the adhesion characteristics of soft coatings on steel substrates - application to Zn-Mg coated steel, Surf. Coat. Technol. 307 ((2016) 1100–1106.
[17] E. Zoestbergen, J. van de Langkruis, T.F.J. Maalman, E. Batyrev, Influence of diffusion on the coating adhesion of zinc-magnesium thin films onto steel, Surf. Coat. Technol. 309 (2017) 904–910.
[18] F.R. Boer, R. Boom, W.C.M. Mattens, A.R. Miedema, A.K. Niessen, Cohesion in Metals: Transition Metals Alloys, North-Holland Physical Publishing, Amsterdam, 1989.
[19] G.M. Song, T. Vystavel, N. van der Pers, J.T. De Hosson, W.G. Sloof, Relation between microstructure and adhesion of hot dip galvanized zinc coatings on dual phase steel, Acta Mater. 60 (2012) 2973–2981.
[20] J. Fornell, S. Gonzalez, E. Rossinyol, S. Surinach, M.D. Baro, D.V. Louzguine-Luzgin, J.H. Perepezko, J. Sorte, A. Inoue, Enhanced mechanical properties due to structural changes induced by devitrification in Fe-Co-B-Si-Nb bulk metallic glass, Acta Mater. 58 (2010) 6256–6266.
[21] A.A.C. Recco, I.C. Oliveira, M. Massi, H.S. Maciel, A.P. Tschiptschin, Adhesion of reactive magnetron sputtered TiNx and TiCy coatings to AISI H13 tool steel, Surf. Coat. Technol. 202 (2007) 1078–1083.